NASA TECHNICAL MEMORANDUM

NASA TM X-52655

NASA TM X-52655

BEHAVIOR OF A VAPOR BUBBLE IN A PULSATING PRESSURE FIELD

N10K-00

by Y. Y. Hsu and R. G. Watts
Lewis Research Center
Cleveland, Ohio

TECHNICAL PAPER proposed for presentation at
Fourth International Heat Transfer Conference
Versailles/Paris, August 31-September 5, 1970

BEHAVIOR OF A VAPOR BUBBLE IN A PULSATING PRESSURE FIELD

by Y. Y. Hsu and R. G. Watts

Lewis Research Center
Cleveland, Ohio

TECHNICAL PAPER proposed for presentation at

Fourth International Heat Transfer Conference
Versailles/Paris, August 31-September 5, 1970

NATIONAL AERONAUTICS AND SPACE ADMINISTRATION

E-5228

BEHAVIOR OF A VAPOR BUBBLE IN A PULSATING PRESSURE FIELD

Y. Y. Hsu and R. G. Watts*
NASA Lewis Research Center, Cleveland, Ohio

Abstract

The response of a vapor-gas bubble to a sinusoidal pressure pulsation is analyzed. The cases of a spherical bubble in an infinite body of liquid and a truncated spherical bubble attached to a wall are examined. The interior of the bubble is assumed to be a mixture of saturated vapor and noncondensable gas. The frequency response function is obtained and includes the effects of frequency, bubble size, and liquid subcooling. Experimental results of bubbles in water and on metal surfaces are compared with the analysis.

INTRODUCTION

Two-phase flow dynamics has been a concern to the heat transfer engineer because of the need to predict or to avoid boiling crisis. It has been shown (refs. 1,2) that premature burnout can result from flow instability in a "soft" system which is highly compressible. The response of void fraction to pressure perturbations is of great importance in analyzing two-phase flow system stability.

The response of gas bubbles to pressure pulsations has been a subject of study in the acoustics field for many years (c.g., refs. 3,4). On the other hand, the behavior of vapor bubbles has only been studied for the case of bubble growth and collapse in a constant pressure field (refs. 5,6,7,8).

The purpose of this study is to examine the response of a vapor bubble in a saturated or near saturated liquid to a pulsating pressure field. The effects of noncondensable gas, bubble shape and the presence of a metallic solid surface will be included in the general analysis. The resulting equations give the amplitude and phase lag of bubble size fluctuation in response to pressure fluctuation. The general equation can be reduced to special cases, such as those for a spherical bubble in a liquid bulk and a hemispherical bubble on a metal surface.

Experiments were conducted to measure the bubble response to sinusoidal pressure pulsations in the above mentioned special cases. The experimental results are compared with the analysis.

ANALYSIS

Formulation

Consider a spherical gas-vapor bubble in an infinite sea of motionless liquid. The geometry of the system is shown in figure 1(a). The temperature of the liquid is assumed to be that for which a gas-vapor bubble of radius R_o with vapor partial pressure P_{vo} and gas partial pressure P_{go} will exist in

*Associate Professor, Mechanical Engineering Department, Tulane University, New Orleans, Louisiana.

equilibrium. If the pressure in the liquid begins to oscillate, the bubble size will oscillate because of the alternate superheating and subcooling of the vapor inside and the expansion and contraction of the gas. It will be assumed that during the oscillations the properties of the liquid remain constant, and that the interior of the bubble is homogeneous with temperature $T_b = T_g = T_v$, pressure $P_b = P_v + P_g$ and density $\rho_b = \rho_v + \rho_g$. The liquid is assumed to be inviscid and incompressible. No heat sources are present. In such a case, the liquid momentum and continuity equations can be combined to yield the Rayleigh equation

$$R \frac{d^2R}{dt^2} + \frac{3}{2} \frac{dR}{dt}^2 = \frac{1}{\rho_l}\left[P_v + P_g - \frac{2\sigma}{R} - P_\infty(t)\right] \quad (1)$$

The energy equation is

$$\frac{1}{\alpha_l}\left(\frac{\partial T_l}{\partial t} + \vec{V} \cdot \text{grad } T_l\right) = \nabla^2 T_l, \qquad r \geq R \quad (2)$$

with boundary conditions

$$T_l(R,t) = T_b$$

$$T_l(r,t) \text{ bounded} \quad (2a)$$

The equation of state for the gas is

$$\frac{dP_g}{P_g} + \frac{dv}{v} = \frac{dT_g}{T_g} \quad (3)$$

The vapor phase is assumed to satisfy the Clausius-Clapeyron relation,

$$dP_v = \frac{h_{fg}}{v_{fg}T_v} dT_v \quad (4)$$

Combining equations (3) and (4) with $T_g = T_v = T_b$ gives

$$\frac{dP_b}{P_g} = \frac{dP_g + dP_v}{P_g} = \left(1 + \frac{h_{fg}}{v_{fg}P_g}\right)\frac{dT_b}{T_b} - \frac{dv}{v} \quad (5)$$

The energy equation for the bubble interior is

$$\overline{mC} \frac{dT_b}{dt} + u_{fg} \frac{dm_v}{dt} + \left(P_b - \frac{2\sigma}{R}\right)\frac{dv}{dt} = k_l A_b \frac{\partial T_l}{\partial r}(R,t) \quad (6)$$

where

$$\overline{mC} = m_v C_{v,v} + m_g C_{g,v}$$

The terms on the left side represent respectively the energy increases in the bubble interior due to sensible heat, internal energy of vaporization, and compression of the gas and vapor. The term on the right side represents heat conduction from the liquid to the bubble interior.

An expression for the rate of evaporation of the vapor must be obtained to complete the formulation. The ratio of masses of vapor and gas in the bubble is

$$\frac{m_v}{m_g} = \frac{M_v}{Z_v M_g}\frac{P_v}{P_g} \tag{7}$$

Since m_g is constant

$$\frac{1}{m_v}\frac{dm_v}{dt} = \frac{1}{P_v}\frac{dP_v}{dt} - \frac{1}{P_g}\frac{dP_g}{dt} \tag{8}$$

Substitution of (5) and (8) into (6) yields

$$\left[\overline{mC} + \frac{u_{fg} m_v P_g}{P_v T_b}\left(1 + \frac{h_{fg}}{v_{fg} P_g}\right) - \frac{u_{fg} m_v P_b}{P_v T_b}\right]\frac{dT_b}{dt}$$

$$+ \left[P_b(1 - W) + \frac{u_{fg} m_v}{v}\right]\frac{dv}{dt} = k_l A_b \frac{\partial T_l}{\partial r}(R,t) \tag{9}$$

Solution

The magnitudes of oscillations of all variables are assumed to be small enough that the system equations can be linearized by defining small dimensionless quantities $x(t)$, $\theta_b(t)$, $\theta_l(r,t)$, $p(t)$, and $\epsilon(t)$, each much smaller than unity, as follows:

$$\left.\begin{array}{ll} R = R_o[1 + x(t)], & T_b = T_o[1 + \theta_b(t)] \\ T_l = T_o[1 + \theta_l(r,t)], & P_\infty = P_o[1 + \epsilon(t)] \\ P_b = P_o[1 + W + p(t)], & W = 2\sigma/R_o P_o \end{array}\right\} \tag{10}$$

Dimensionless time and distance functions are defined as

$$\tau = \alpha_l t/R^2, \qquad y = r/R_o \tag{11}$$

When the quantities defined in equations (10) and (11) are substituted into (1), (2), (5), and (9) and terms involving products of small quantities are neglected, the following equations result:

$$\frac{d^2x}{d\tau^2} - BWx = B(p - \epsilon) \tag{12}$$

$$\frac{\partial^2}{\partial y^2}(y\theta_l) = \frac{\partial}{\partial \tau}(y\theta_l) \tag{13}$$

$$\left.\begin{array}{l} \theta_l(1,\tau) = \theta_b(\tau) \\ \theta_l \text{ is bounded} \end{array}\right\} \tag{13a}$$

$$p = \frac{P_{go}}{P_{bo}}\left(1 + \frac{h_{fg}}{v_{fg} P_{go}}\right)\theta_b - 3\frac{P_{go}}{P_{bo}}x \tag{14}$$

$$K_1 \frac{d\theta_b}{d\tau} + K_2 \frac{dx}{d\tau} = \frac{\partial \theta_l}{\partial y}(\tau,1) \tag{15}$$

where

$$B = P_o R_o^2 / \rho_l \alpha_l^2$$

$$K_1 = \frac{C_v \rho_v}{3 C_l \rho_l} \left[1 + \frac{C_g M_g}{C_v M_v} \frac{P_{go}}{P_{vo}} + \frac{u_{fg}}{C_v T_o} \left(\frac{h_{fg}}{v_{fg} P_v} - 1 \right) \right] \tag{15a}$$

$$K_2 = \frac{\mathcal{R} \rho_{go}}{C_l M_g \rho_l} (1 - W) + \frac{\rho_v}{\rho_l} \left(\frac{u_{fg}}{C_l T} \right)$$

Equations (12) to (15) constitute a set of linear differential equations relating the dimensionless pressure variation $\epsilon(t)$ to the dimensionless change in bubble radius $x(t)$. It is shown in standard books on linear system theory that if such a system is excited by an oscillatory input, the response will be oscillatory. The ratio of the magnitudes of the output and input variables is given by the magnitude of the frequency response function, which is the ratio of the Laplace transforms of the output and input variables with zero initial conditions and with the Laplace variable S set equal to the imaginary dimensionless frequency

$$j\Omega = j\omega \left(R_o^2 / \alpha_l \right) .$$

Solution of equations (12) to (15) for the ratio $\mathcal{L}\{x(t)\}/\mathcal{L}\{\epsilon(t)\} = X(s)/E(s)$ is straightforward and the details will not be discussed here. The corresponding frequency response function is

$$\frac{X(j\Omega)}{E(j\Omega)} = \frac{1}{W - 3\left(\frac{P_{go}}{P_{bo}}\right)(1 + W) + \left(\frac{\rho_l \alpha_l^2}{P_o R_o^2}\right)\Omega^2 - \left(\frac{h_{fg}}{v_{fg} P_{bo}} + \frac{P_{go}}{P_{bo}}\right)\left[\frac{K_2 (1 + W) j\Omega}{1 + \sqrt{j\Omega} + K_1 j\Omega}\right]} \tag{16}$$

Since X/E represents the ratio of the dimensionless radius change to the dimensionless pressure variation, it can be called the dimensionless compressibility of a bubble.

Bubble on a Wall

If the bubble rests against a solid wall (fig. 1(b)), heat conduction takes place through the liquid and also through the wall. The bubble is assumed to be a segment of a sphere, and equations (12) to (14) still hold true. The bubble energy equation (15) must be altered to include heat conducted through the solid wall. This equation becomes

$$K_1 \frac{d\theta_b}{d\tau} + K_2 \frac{dx}{d\tau} = \frac{\partial \theta_l}{\partial y}(1,\tau) + \frac{k_w A_w}{k_l A_b} \frac{\partial \theta_w}{\partial \zeta}(0,\tau) \tag{17}$$

The heat conduction equation for the solid wall must also be accounted for. In dimensionless form,

$$\frac{\alpha_l}{\alpha_w} \frac{\partial \theta_w}{\partial \tau} = \frac{\partial^2 \theta_w}{\partial \zeta^2} \tag{18}$$

Boundary conditions are taken as

$$\theta_w(0,\tau) = 0, \qquad \frac{\partial\theta_w}{\partial\zeta}\left(\frac{L}{R_o},\tau\right) = 0 \tag{18a}$$

When these changes are made the modified form of the frequency response function is

$$\frac{X(j\Omega)}{E(j\Omega)} =$$

$$\frac{1}{W-3\,\frac{P_{go}}{P_{bo}}(1+W)+\frac{\rho_l\alpha_l^2\Omega^2}{P_oR_o^2}-\left(\frac{h_{fg}}{v_{fg}P_{bo}}+\frac{P_{go}}{P_{bo}}\right)\left[\frac{jK_2\Omega(1+W)}{1+K_1j\Omega+\sqrt{j\Omega}\left(1+\frac{k_wA_w}{k_lA_b}\sqrt{\frac{\alpha_l}{\alpha_w}}\tanh\sqrt{\frac{j\Omega\alpha_l L}{\alpha_w R_o}}\right)}\right]} \tag{19}$$

When $L\alpha_l\Omega/R_o\alpha_w$ is large,

$$\frac{X(j\Omega)}{E(j\Omega)} = \frac{1}{W-3\,\frac{P_{go}}{P_{bo}}(1+W)+\frac{\rho_l\alpha_l^2\Omega^2}{P_oR_o^2}-\left(\frac{h_{fg}}{v_{fg}P_{bo}}+\frac{P_{go}}{P_{bo}}\right)\left[\frac{jK_2\Omega(1+W)}{1+K_1j\Omega+\sqrt{j\Omega}\left(1+\frac{k_wA_w}{k_lA_b}\sqrt{\frac{\alpha_l}{\alpha_w}}\right)}\right]} \tag{20}$$

EXPERIMENTAL APPARATUS AND PROCEDURE

The experimental apparatus consists of a test cell, a pressure pulse generating device, a camera, and a data recording device (fig. 2).

The test cell is a cylindrical tank with an optically-flat front window. The cell is connected to the pulse generator and the pressure transducer at the bottom. A vent is located at the top of the circular sidewall to eliminate vapor (or gas) pockets. A nylon net with fine mesh was used to trap the vapor bubbles for study of bubbles in the bulk. Metal blocks (about 2.5 cm inside), of copper and stainless steel were used for study of bubbles on metallic surfaces. The undersurfaces of these specimens were concaved slightly to trap bubbles. A 100-watt heater was situated under the surfaces to keep the water warm and to supply vapor bubbles. Additional heat was supplied by infrared lamps. The unexposed sides were insulated.

The pulse generator was a four-way valve made to rotate. The four ports were connected to the laboratory low pressure air line, vacuum line, atmosphere and test cell (through a surge tank). The test cell was thus alternately exposed to positive and negative pressures, and a smooth sinusoidal pressure wave was obtained. The frequency is adjustable through changing the rotating speed of the valve over a limited range of 1 to 4 cycles per second.

The thermocouple readings of the bulk and the metal specimens and the transducer readings were monitored by a digital voltmeter. Temperature could be read to within 0.2° C accuracy. But due to the slight nonuniformity of temperature field in the cell, the accuracy of temperature data is probably no better than 1° C. Pressure could be read to within 1 cm of water column.

For synchronization purposes, both the camera and the recorder were provided with 100 cps timing marks. A zero-time lamp was put in front of the camera. When the lamp turned off a galvanometer reading would deflect on the oscillograph chart. These two events are taken as zero-time.

During each run, while data was being taken, the heater was turned off to ensure clean sinusoidal pressure waves. Otherwise, the heater would generate a large number of bubbles, thus imposing random pressure pulses onto the primary pressure wave.

RESULTS AND DISCUSSION

Presentation of Results

Figures 3, 4, and 5 are comparisons between experimental and analytical results for bubbles in the bulk, on the copper surface, and on the stainless steel surface. Curves are plotted for the case $R_o = 10^{-1}$ centimeter. The effect of radius is felt only at very high frequencies, however, and curves at other R_o values would be almost indistinguishable from those given in the frequency range shown.

Controlling Mechanisms

The analytical equations (16), (20) have incorporated the effects of inertia, heat transfer, and surface tension. Close examination of the relative magnitudes of the various terms using properties of water reveals that the bubble response is inertia-controlled in the high frequency range ($\Omega > 10^5$) and heat transfer-controlled in the low frequency range ($\Omega < 10^3$). This is consistent with the bubble dynamic analysis for the constant pressure field (e.g. in nucleate boiling, cavitation, etc.) in which it is generally accepted that bubble growth rate is inertia-controlled only in the very early stage ($t < 10^{-5}$ sec) but is heat transfer-controlled throughout most of the bubble life ($t > 10^{-2}$ sec).

For the size of bubbles and the frequency range encountered in the experimental study, Ω is usually in the range of 10^1 to 10^3. In this range, heat transfer is the controlling mechanism.

Effect of Frequency

The qualitative trend of figures 3, 4, and 5 shows that when bubbles contain only vapor ($T_b = 373°$ K for water under 1 atm), the amplitude response of the bubbles is strongly dependent upon the dimensionless frequency Ω. These bubbles are highly compressible in the lower Ω range and become far less compressible at high dimensionless frequency. This behavior can be explained by consideration of the heat transfer mechanisms. The dimensionless frequency, by definition, is the ratio of the thermal diffusion time, R_0^2/α to the pulsation period. Therefore, when the dimensionless frequency is large, the time available during a compression or expansion period is insufficient for heat to diffuse through the liquid and the bubble behaves nearly adiabatically. In such a case the mass transfer due to latent heat exchange is small and the condensable vapor behaves similarly to the noncondensable gas. On the other hand, at lower frequencies case, a long period is available for the heat to diffuse. Thus, latent heat involved with condensation can be exchanged back and forth between the bubble and the liquid. The accompanying mass transfer gives rise to large bubble pulsations. When even a small amount of noncondensable gas is present in the bubble, the dependence of compressibility on frequency is greatly diminished.

Effect of Noncondensable Gas

The effect of noncondensable gas is shown by the lines marked with bulk temperature. It was observed that noncollapsable bubbles could be obtained and maintained indefinitely in subcooled water. This indicates the presence of noncondensable gas in the bubble in addition to the vapor. Assuming that the partial pressure of the vapor can be expressed by the vapor pressure along the saturation curve, the balance of the partial pressure must be contributed by gas dissolved in the water which was released into the bubble. Thus, a bubble in the subcooled liquid contains a mixture of vapor and gas, with the composition of gas increasing with increasing subcooling. The analytical lines showed that a trace amount of gas (or a very small subcooling), could mean an order of magnitude drop in amplitude response. The experimental data for near saturation condition lay in between the saturation curve and 1° C subcooling curve. While the 2° C subcooled data lay just below the corresponding 371° K line. This result tends to substantiate the analysis. It also shows how much one could be in error if a trace amount of noncondensable gas is discounted as negligible. It should be emphasized that in the present study, the bubble interior is assumed to be homogeneous. Thus, retardation of diffusion of vapor caused by the noncondensable gas is neglected. This is justified on the grounds that mass diffusion due to the change of phase for a pulsating bubble takes place in alternate directions, and thus it would not cause an accumulation of inert gas to form a diffusion barrier as observed in the film condensation studies (ref. 9).

Effect of Surface

The presence of a solid surface provides another avenue for heat to be transferred in and out of the bubble. In this analysis, it is assumed that the liquid film between the bubble and the solid surface is so thin that it does not offer any resistance to heat transfer. Such an assumption might be vulnerable for the case of high frequency. For the low frequency range, the experimental results appear to agree with the analysis reasonably well. It should be noted that, in this study, thick blocks of metals were used. Therefore, only the effect of conductivity and thermal diffusivity can be studied. To this effect, the results show that bubbles on copper are more compressible than stainless steel which is less conducting. Equation (19) indicates (without experimental verification) that the thickness of the metal wall could be a factor too. Thus, the void response in a tube to a pressure pulse could very well depend upon the tube thickness as well as the tube material.

The presence of metal surface effects the dimensionless compressibility more strongly when the liquid temperature approaches saturation temperature (i.e., near all-vapor condition). The effect of a solid surface diminishes as gas content is increased with increasing subcooling.

Effect of Bubble Shape

The bubble shape does not appear to greatly alter the compressibility. Apparently due to the fact that the ratio v/A_b does not vary over a very great range (e.g., for the same volume, the surface areas of spherical bubble and a hemispherical bubble differ only by 20 percent). Thus, for estimation purpose, a spherical bubble could be assumed without introducing a large error.

CONCLUSION

The dynamic response of a vapor bubble to a sinusoidal pressure pulsation was studied both analytically and experimentally, for the cases of bubbles in the liquid bulk and on metal surfaces. The studies showed that bubble response is strongly dependent on the frequency and gas content. It is also dependent on the thermal properties of the metal but is only weakly dependent on the bubble shape. The analysis also showed that the bubble dynamics are inertia controlled in the high frequency range but thermal-controlled in the low frequency range.

NOMENCLATURE

A	area
B	a dimensionless parameter defined in equation (15a)
C	specific heat
E	$\Delta P/P_o$
h_{fg}	latent heat of evaporation
j	$\sqrt{-1}$
k	thermal conductivity
K_1	dimensionless parameter defined in equation (15a)
K_2	dimensionless parameter defined in equation (15a)
L	thickness of solid wall
M	molecular weight
m	mass
P	pressure
p	small perturbation in pressure, dimensionless, equation (10)
R	bubble radius
r	coordinate as shown in figure 1

T	temperature
t	time
u	internal energy
$\vec{V}$	velocity
v	volume
v_{fg}	change of specific volume due to evaporation
W	Weber number, defined in equation (10)
X	$\Delta R/R_o$
x	small perturbation in radius, dimensionless, equation (10)
y	dimensionless radius coordinate, equation (11)
Z	compressibility coefficient
z	coordinate, figure 1(b)
α	thermal diffusivity
ϵ	small perturbation in pressure, dimensionless, equation (10)
θ	small perturbation in temperature, dimensionless, equation (10)
σ	surface tension
ρ	density
ζ	dimensionless coordinate, Z/R_o
τ	dimensionless time, equation (11)
Ω	dimensionless frequency, $2\pi/\tau$

Subscripts:

b	bubble
fg	change from liquid to vapor
g	gas
l	liquid
o	unperturbed value
v	vapor, also constant volume
w	wall
∞	infinity

REFERENCES

[1] M. Silvestri: Fluid Mechanics and Heat Transfer of Two-Phase Annular-Dispersed Flow. Advances in Heat Transfer, Vol. 1, T. F. Irvine, Jr. and J. P. Hartnett, eds., Academic Press, New York, pp. 355/446 (1964).

[2] I. T. Aladyev, L. L. Miropolsky, V. E. Doroshahuk, and M. A. Styrikovich: Boiling Crisis in Tubes. International Developments in Heat Transfer, ASME, New York, pp. 237/243 (1963).

[3] C. Devin, Jr.: Survey of Thermal, Radiation, and Viscous Damping of Pulsating Air Bubbles in Water. J. Acoust. Soc. Am., vol. 31, no. 12, pp. 1654/1667 (1959).

[4] D.-Y. Hsieh and M. S. Plesset: Theory of Rectified Diffusion of Mass Into Gas Bubbles. J. Acoust. Soc. Am., vol. 33, no. 2, pp. 206/215 (1961).

[5] M. S. Plesset and S. A. Zwick: The Growth of Vapor Bubbles in Superheated Liquids. J. Appl. Phys., vol. 25, no. 4, pp. 493/500 (1954).

[6] H. K. Forster and N. Zuber: Growth of a Vapor Bubble in Superheated Liquid. J. Appl. Phys., vol. 25, no. 4, pp. 474/478 (1954).

[7] S. G. Bankoff and R. D. Mikesell: Growth of Bubble in a Liquid of Initially Non-Uniform Temperature. ASME Paper No. 58-A-105 (1958).

[8] L. W. Florschuetz and B. T. Chao: On the Mechanics of Vapor Bubble Collapse. J. Heat Transfer, vol. 87, no. 2, pp. 209/220 (1965).

[9] D. G. Kroger: Heat Transfer During Film Condensation of Potassium Vapor. Massachusetts Inst. Tech. Report DSR 75239-42 (1966).

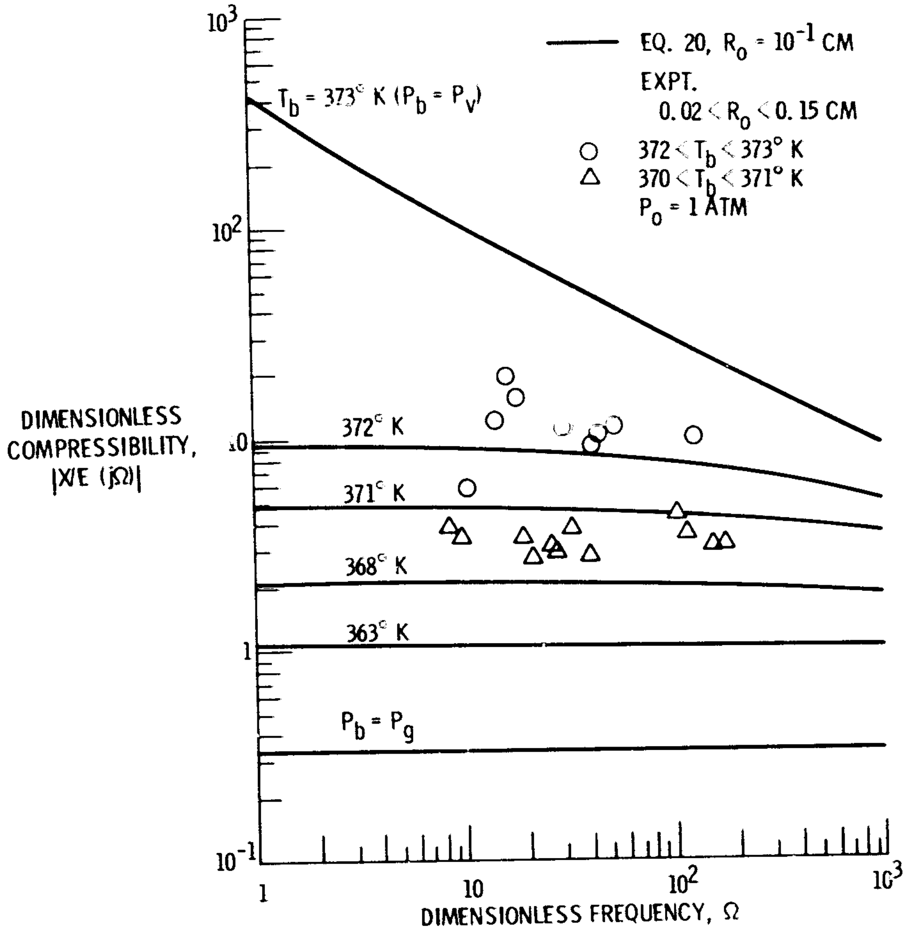

Figure 4. - Dimensionless compressibility of water-air bubbles on stainless steel surface.

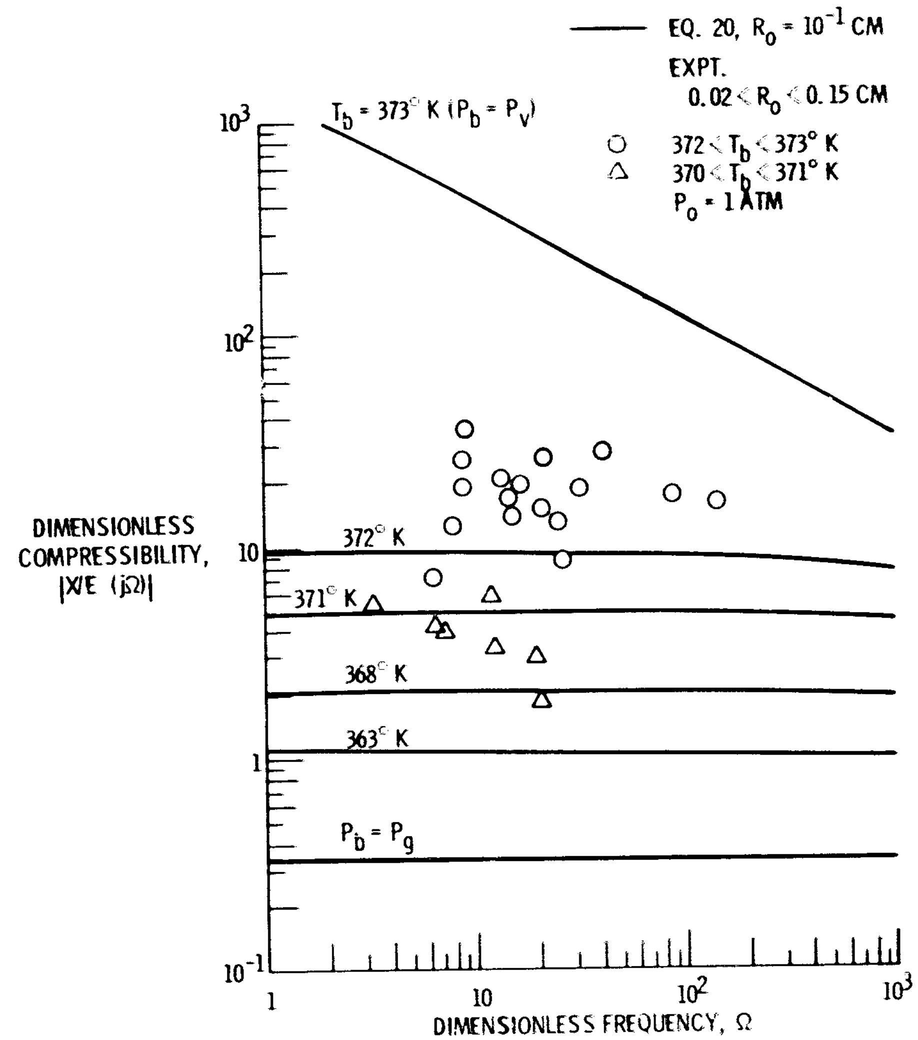

Figure 5. - Dimensionless compressibility of water-air bubbles on copper surface.